THE ASTROPHYSICAL JOURNAL, 566:261–266, 2002 February 10
© 2002. The American Astronomical Society. All rights reserved. Printed in U.S.A.

METASTUDY OF THE SPIRAL STRUCTURE OF OUR HOME GALAXY

JACQUES P. VALLÉE
National Research Council of Canada, Herzberg Institute of Astrophysics, 5071 West Saanich Road, Victoria, BC V9E 2E7, Canada; jacques.vallee@nrc.ca
Received 2001 May 7; accepted 2001 October 10

ABSTRACT

The current maps of the Milky Way disk still have large differences, much like early maps of the Earth's continents made in the 16th century had sizeable differences in the locations of continents and many areas labeled "terra incognita." Exactly where are the spiral arms in our home Galaxy (in radius and longitude)? Here a meta-analysis is made of the recent (1995–2001) observational data on the pitch angle (p) and the number (m) of spiral arms in our home Galaxy. In order to clarify our image of the structure of the Milky Way, logarithmic model arms of the form $\ln(r/r_0) = k(\theta - \theta_0)$ are fitted to the observed tangents to the spiral arms and to the observed position angle (P.A.) of the Galaxy's central bar. The main results are that $p = 12°$ inward and $m = 4$, with logarithmic spiral arm parameters $r_0 =$ 2.3 kpc and $\theta_0 = 0°$ for the Norma arm. The value of θ_0 for the other three arms is modeled by rotating the Norma arm in steps of 90°. These values are similar to those found by Ortiz & Lépine using earlier observational data, with some differences. The best model predicts an interarm distance near the Sun of $S = 2.5$ kpc (from the Sagittarius to the Perseus arm) and a distance from the Sun to the Sagittarius arm of 0.9 kpc. These values are compared to our limited and uncertain data from the observed nearby spiral arms. These predicted values near the Sun differ substantially from the predictions of Ortiz & Lépine, as discussed in the text.

Subject headings: Galaxy: disk — Galaxy: fundamental parameters — Galaxy: structure — ISM: general — ISM: structure

1. INTRODUCTION

Previous attempts at fitting logarithm spirals to spiral galaxies have been made. Thus, using observational data up to 1993, Ortiz & Lépine (1993) modeled four such arms and predicted the star counts at infrared wavelengths for our Galaxy. In addition, using the results published in the period 1980–1994, a metastudy of 15 papers indicated that our home Galaxy may have $m = 4$ arms, with a mean pitch angle $p = 12°$ inward (Vallée 1995), and there was some controversy since a minority of these studies indicated $m = 2$ arms with a lower pitch angle.

In other spiral galaxies, observations have shown a number $m = 1, 2, 3, 4$, and even 5 spiral arms, with galaxies having odd m values being rarer (see Elmegreen, Elmegreen, & Montenegro 1992). Being within the disk of our home Galaxy the Milky Way and having very little data from the other side of the Galactic center (GC), there is then an emphasis here on getting many different tracers on our side of the Galaxy in order to project a better global picture.

Aim of this paper.—Since 1995, a large number of new observational results have been published, warranting a fresh look at this issue. In addition, firmer conclusions have appeared concerning some aspects of Galactic research relevant to spiral structure as observed from the Sun's location: the presence of a central bar, and the GC distance. These parameters need to be incorporated in any model revision. In this paper, a meta-analysis is made for the mean values of the observed global parameters of the home Galaxy (m, p). Together with the observed arm tangents and bar P.A., a logarithmic model is employed to yield the best locations (radius, longitude) for the spiral arms in the Milky Way disk. From the best fit, predictions are made notably for the most likely interarm separation S near the Sun and for the Sun's distance to the Sagittarius arm.

Within 3 kpc of the GC, there is a rotating bar straddling the nucleus, oriented in the first quadrant about $20° \pm 6°$ from the Sun–GC axis, as also derived from analysis of near-infrared light, H I, CO, and CS molecular data, diffuse near-infrared background, and other tracers (Freudenreich 1998; Binney et al. 1991). The bar ends at 3 kpc from the GC, at the edge of a circumscribing molecular/stellar ring, with spiral arms beginning at points on the ring, possibly along and across the bar's major axis (Freudenreich 1998). There is considerable discussion about the central bar's parameters (see recent summaries in Fux 2001 and Gerhard 1999). The central bar could affect any interpretation of putative spiral arms close ($-18° < l < 18°$) to the direction of the GC (e.g., Fig. 4 in Ortiz & Lépine 1993).

For the distance from the Sun to the GC, the IAU in 1986 recommended 8.5 kpc from indirect measurements. Direct proper-motion measurements showed this distance to be 7.2 ± 0.7 kpc (Reid 1993). Consistency requirements, using H II and H I radial velocity data and others fitted to rotation curves, showed that a consistent picture emerges only for a Sun–GC distance of 7.1 ± 0.4 kpc (Ollin & Merrefield 1998). There is considerable discussion about this value (see Paczyński & Stanek 1998). Favoring consistency models and direct measurement, here I adopt a mean value of 7.2 ± 0.4 kpc.

In § 2, I assemble the data since 1995, discuss them as to their overall quality, and use statistics on the recent results pertaining to the Galactic structure (arms and pitch angle). In § 3, models of spiral arms are drawn, with the mean pitch angle and number of arms as found here; then a model fit is made to the observations of the tangents to the known spiral arms (within their errors), and the results of the fits are employed to predict the present interarm distance near the Sun, and the Sun's separation to the Sagittarius arm. A concluding discussion on these predictions follows in § 4.

TABLE 1

RECENT STUDIES OF SPIRAL ARMS IN THE MILKY WAY (1995–2001)[a]

Inward Pitch Angle	Number of Spiral Arms	Figure and Reference	Observational Data Used	Relative Weight (Best = 3)
14°	4	Fig. 2 in Johnston et al. (2001)	H I gas	2
... .	4	Steiman-Cameron, Wolfire, & Hollenbach (2001)	[C II], [N II]	2
06°	2	Fig. 4 in Fernandez et al. (2001)	Cepheids, OB stars	1
14°	4	Fig. 4 in Fernandez et al. (2001)	Cepheids, OB stars	1
06°, 12°	6	Fig. 6 in Lépine et al. (2001)	Cepheids, H II gas	1
20°	4	Fig. 12 in Vallenari, Bertelli, & Schmidtobreick (2000)	V, I optical stars	2
13°	4	Fig. 1 in Drimmel (2000)	Dust 240 μm	2
17°	2	Fig. 2 in Drimmel (2000)	*K*-band old stars	2
14°	4 outer	Fig. 16 in Fux (1999)	H I, CO gas	3
11°	4	Table 1 in Mishurov & Zenina (1999)	Cepheids	2
06°	2	Table 1 in Mishurov & Zenina (1999)	Cepheids	1
11°	4	Fig. 15*b* in Englmaier & Gerhard (1999)	H I, CO, NIR COBE	2
09°	4 outer	Fig. 14 in Sevenster (1999)	OH, IR stars	2
08°	4	Fig. 4 in Han, Manchester, & Qiao (1999)	RM pulsars	1
07°	4	Fig. 1 in Indrani & Deshpande (1999)	RM pulsars	1
11°	4	Fig. 3 in Efremov (1998)	H I clouds	2
14°	4	Fig. 4 in Amaral & Lépine (1997)	Nearby open clusters	1
07°	...	Table 3 in Heiles (1996)	Polarized stars	1
17°	4	Fig. 1 in Chen et al. (1996)	^{26}Al 1.8 MeV	2
17°	4	Fig. 1 in Deshpande (1995)	Radio pulsars	1
11.7 ± 1.0 [b].....	3.8 ± 0.3[b]	...	...	...

[a] See Table 1 in Vallée 1995 for papers in the period 1980–1994.
[b] Unweighted mean value and standard deviation of the mean.

2. OBSERVATIONS

2.1. *Data and Evaluation*

A search of NASA's Astrophysics Data System was made for all papers published on this topic since 1995. While incomplete for some journals, the results are representative of the whole and cover 100% of the main journals.

Table 1 lists chronologically the results found in the literature, giving for each one the pitch angle found, the number of arms, the reference and most telling figure, the type of observational data used, and a relative weight (as explained below).

For the purpose of evaluation, a relative weight of 2 is assigned to these studies, except as otherwise noted below. A worse weight of 1 is assigned if the method used or study is limited to the local area (near the Sun) or is more indirect (more assumptions), and a better weight of 3 is assigned if the method or study encompassed many arm tracers and included multiple models.

2.2. *New Statistics*

Figure 1 shows the histogram for the pitch angle p of the arms. Because each arm-tracer method has its own corrections to perform (e.g., dust contamination at optical wavelengths) and can still have undiscovered calibration effects to be sorted out later, at this time it is best to use several different tracers of spiral arms and then perform a statistical analysis on the whole (meta-analysis, or statistical analysis of a group of experiments to determine the overall significance of an effect).

Since most studies find that $m = 4$ (i.e., 15 of 19 studies in Table 1), I can first select the $m = 4$ studies only and use the relative weights in the last column of Table 1 to obtain the weighted statistical results for the studies in the period 1995–2001 as follows: $p = 13.1 \pm 0.7$. As a check, I can take all 19 studies (with $m = 2, 4, 6$) and obtain the weighted statistical results in that same period as $p = 12.4 \pm 0.7$. For all 19 studies in the same period, the unweighted results are given in the last row of Table 1, as $p = 11\overset{\circ}{.}7 \pm 1\overset{\circ}{.}0$ and $m = 3.8 \pm 0.3$.

The unweighted results for the period 1995–2001 in Table 1 are independent of the unweighted results for the 16

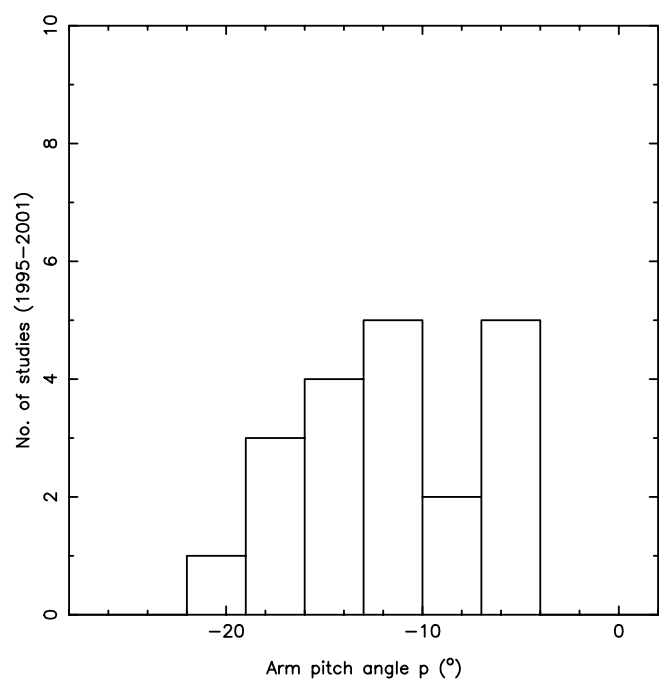

FIG. 1.—Histogram of the number of studies (*vertical axis*) yielding the pitch angle values shown.

studies published in the period 1980–1994 ($p = 11.^\circ6 \pm 1.^\circ4$ inward and $m = 3.4$, in Vallée 1995). The new results are about the same as the old ones within their combined errors, indicating the consistency of the two independent metastudies using two different time periods (1980–1994; 1995–2001). Given the small range of these results, with mean p values from $11.^\circ7$ to $13.^\circ1$, I shall use $p = 12^\circ$ and $m = 4$ in what follows.

3. MODELING WITH LOGARITHMIC SPIRAL ARMS

3.1. *Logarithmic Models*

Most published models of spiral galaxies employ simple curves. The logarithmic spiral has a constant pitch angle at different radii and is thus independent of radial scale. In most cases, observations of arms in normal spiral galaxies are well represented by logarithmic spirals (Grosbol 1994). For the logarithmic curves, the model adopted here uses equation (1) given in Vallée (1995), with integer values $m = 4$ and an inward pitch angle of 12° (from Table 1).

For the coordinate system, I use a simple (x, y) system with the origin at the GC (where $x = 0$, $y = 0$), with the y-axis toward the Sun (the Sun is at $x = 0$, $y = 7.2$ kpc) and with the x-axis to the right (perpendicular to the y-axis, parallel to $l = 90^\circ$).

For each spiral arm, the equation reduces to four similar curves, each rotated by 90°, of the generic form

$$x = r \cos \theta \; ; \quad y = r \sin \theta \; ; \quad r = r_0 e^{kz}; \qquad (1)$$

with θ measured counterclockwise from the x-axis (horizontal, perpendicular to the Sun–GC line). The direction to the Sun has an angle $\theta = 90^\circ$ from the x-axis, and the Galaxy's central bar is inclined at an angle $\theta = 70^\circ$ from the x-axis. In equation (1), one has that $z = (\theta - \theta_0) > 0$, in radians; $k = \tan(p)$ ($k = 0.2126$ from Table 1); $r_0 =$ constant (obtained by a proper fit to the observations); and $\theta_0 =$ constant (obtained by a proper fit to the observations).

Model arm data lying outside a specific physical range (below $r = 3$ kpc and above $r = 13$ kpc) are not used, because of other physical phenomena occurring there (bar and nucleus; warp and tides).

3.2. *The Observed Tangents and the Central Bar's Position Angle*

To constrain r_0 and θ_0, two independent observational parameters are needed. I choose the relevant ones to be (1) the predicted versus observed tangents to the spiral arms (in Galactic longitude) as seen from the Sun's location and (2) the physical need for two spiral arms to join the two ends of the observed central bar, given the observed P.A. of the bar with respect to the Sun–GC line.

The adopted mean values of the Galactic longitude of the tangents to five long portions of spiral arms are given in Table 1 of Englmaier & Gerhard (1999). That table does not contain some putative inner arms very close with $-18^\circ < l < 18^\circ$ and within 3 kpc of the GC (e.g., Table 1 in Ortiz & Lépine 1993) because these objects would be affected by the central bar and may still be spurs. The adopted mean value of the P.A. of the central bar is given in the Introduction.

By taking a set of values (r_0 and θ_0), one can plot the resulting arms and compare the predicted arm tangents and bar P.A. A very good model fit was found to these observational data, to within 3°, comparable to the observational errors, for $r_0 = 2.3 \pm 0.1$ kpc and $\theta_0 = 0^\circ \pm 3^\circ$. This corresponds to the Norma arm, starting in the vicinity of one end of the central bar.

Owing to a similarity condition, the Perseus arm has $\theta_0 = -270^\circ$, the Sagittarius arm has $\theta_0 = -180^\circ$, and the Scutum arm has $\theta_0 = -90^\circ$ (all negative to preserve the conditions $z > 0$).

Figure 2 shows the result of the fit, showing the best locations of the spiral arms, given the constraints on m and p (Table 1), on the arm tangents, and on the central bar's P.A. The Sun is set at 7.2 kpc from the GC. The area on the other side of the GC has been darkened, owing to our poor observational knowledge there ("zona Galactica incognita").

This model resembles substantially the one used in Ortiz & Lépine (1993), with a logarithmic equation, use of the tangential fits, and values found for the basic parameters. Table 2 shows a comparison of the two models. However, the observational input data come from different epochs (1995–2001 versus 1993 and before). In addition, the two models differ in the use or not of the spurs and bar close to the GC (see above). Also, the predictions start to differ substantially at large radial distances ($r > 6$ kpc).

3.3. *Interarm Distance*

From the model fit above, one can predict the interarm distance near the Sun (along the line Sun–GC), as follows. The predicted radial separation S between different arms (for adjacent arms), or the radial distance between one arm

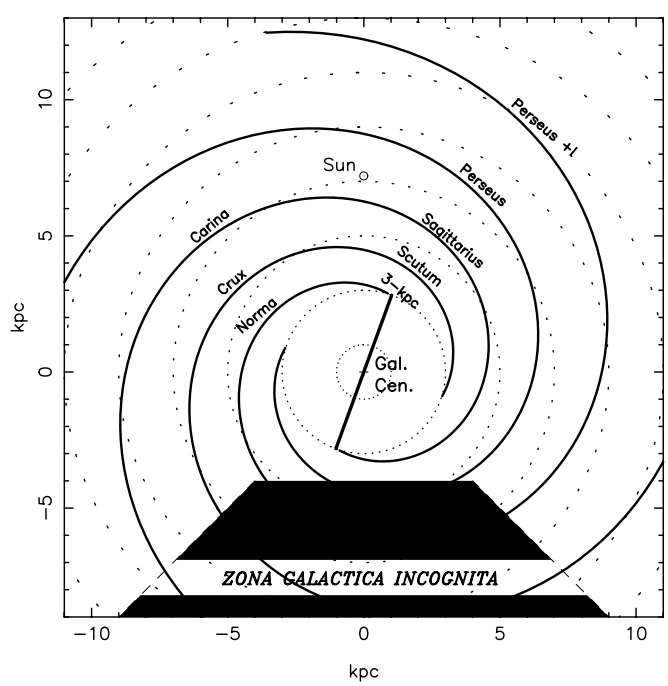

FIG. 2.—Model of logarithmic spiral arms, using the results of this metastudy ($p = 12^\circ$ inward, $m = 4$). The logarithmic model was fitted to the Galactic longitude values of the tangents to the observed spiral arms as seen from the Sun. The Sun is shown by a circled dot, with the Sun–GC distance taken as 7.2 kpc (y-axis). A central bar extends radially from the GC to 3 kpc, inclined clockwise at an angle of 20° to the Sun–GC line. Dots show concentric circles around the GC, at a Galactic radius $r = 1, 3, 5, 7, 9, 11, 13$ kpc.

TABLE 2

COMPARISON OF TWO LOGARITHMIC SPIRAL MODELS

Model	This Paper	Ortiz & Lépine (1993)
Input Data:		
Pitch angle data (period)	1995–2001	Up to 1993
Observed tangents to the arms (reference)	Table 1 in Englmaier & Gerhard (1999)	Table 1 in Ortiz & Lépine (1993)
Galactic central bar P.A.[a]	$20° \pm 6°$	(None used)
Sun to Galactic center distance	7.2 ± 0.4 kpc	7.9 kpc
Meta-Analysis:		
p (inward)	$12° \pm 1°$	13°.8
m	4	4
Model Parameters:		
r_0	2.3 ± 0.1 kpc	2.3 kpc
θ_0	$0° \pm 3°$	0°
Predictions:		
Interarm separation at Sun	2.5 ± 0.3 kpc	3.7 kpc (their Fig. 4)
Sun to Sagittarius arm	0.9 ± 0.4 kpc	0.3 kpc (their Fig. 4)

[a] Measured at the GC, starting clockwise from the Sun–GC axis.

and the next arm, is given by equation (7) in Vallée (1995) as

$$2\pi \tan p = m \ln\left(1 + \frac{S}{r_1}\right). \quad (2)$$

For the mean values $m = 4$, $p = 12°$, one gets $S/r_1 = 0.40$. Using r_1 seen on Figure 2 as the distance from the GC to the Sagittarius arm (along the Sun–GC line), one gets $S = 0.40 r_1 = 2.5$ kpc.

Similarly, using the logarithmic equation (1) above, with the Sun–GC line at $\theta = 90°$ and the parameters of fit $r_0 = 2.3$ kpc, for the Sagittarius arm $\theta_0 = -180°$ one gets $r_1 = 6.26$ kpc, while for the Perseus arm $\theta_0 = -270°$ one gets $r_2 = 8.75$ kpc. This gives $S = r_2 - r_1 = 2.5$ kpc.

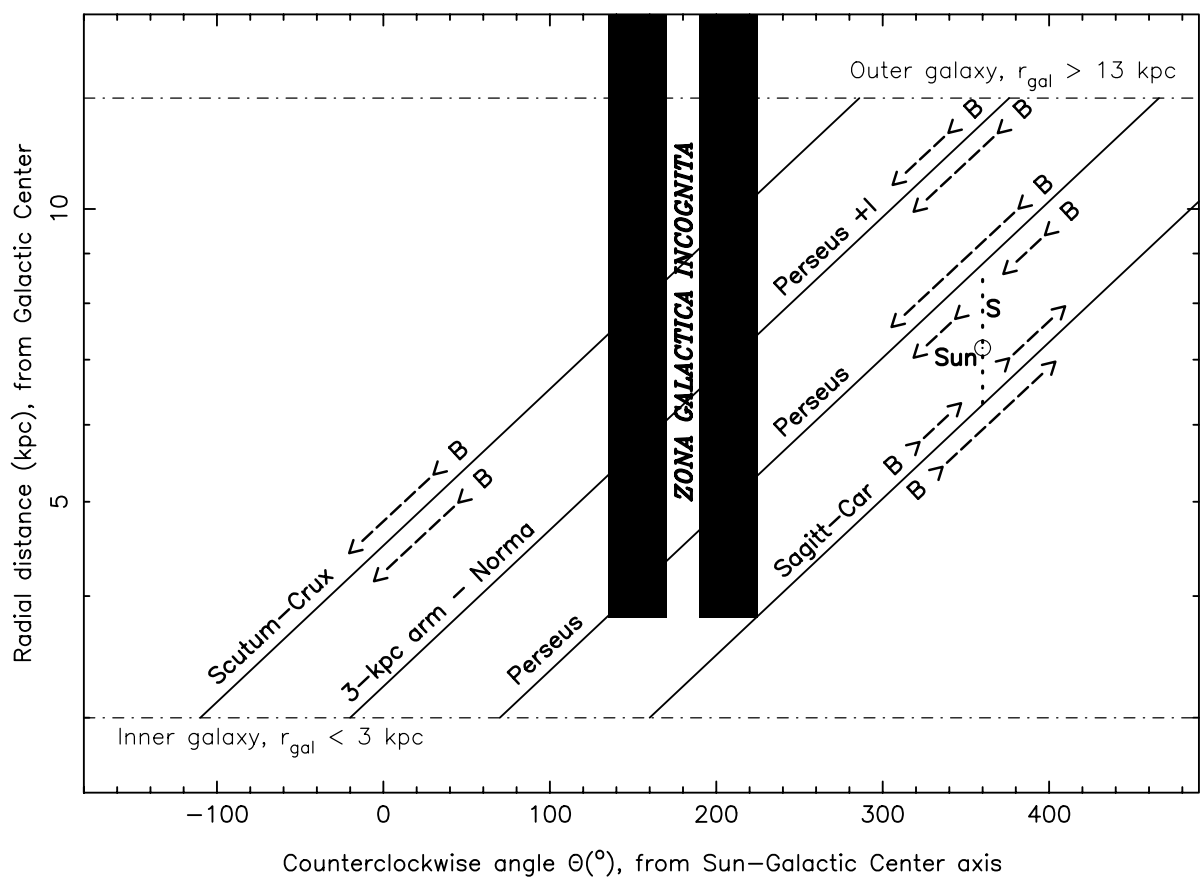

FIG. 3.—Image of the unwrapped spiral arms in our home Galaxy ($m = 4$, $p = 12°$ inward). For each arm, the log of the radial distance (*vertical axis*) is given as a function of the azimuthal angle from the Sun–GC line (measured counterclockwise as seen from the north Galactic pole). The Sun is shown by a circled dot ($\theta = 360°$, $r = 7.2$ kpc). The interarm distance S through the Sun is shown vertically. The observed Galactic magnetic field directions are drawn with arrows (data from Fig. 9 in Vallée 1997).

In addition, the predicted distance of the Sun to the Sagittarius arm at r_1 is $7.20 - 6.26 = 0.94$ kpc.

4. DISCUSSION

4.1. *Interarm S*

Is this interarm prediction $S = 2.5$ kpc reasonable? A look at the references in Table 1 indicates an observational range of S values, from 0.5 kpc (Lépine, Mishurov, & Dedikov 2001) to 3.5 kpc (Johnston et al. 2001).

Similarly, the Sun's distance to the Sagittarius arm is claimed observationally to be from 0.3 kpc (Ortiz & Lépine 1993) to 1.2 kpc (Johnston et al. 2001).

The Cepheids method could be reliable when thoroughly calibrated and all biases are taken out. Using only Cepheid stars located outside the local Gould Belt (i.e., outside 0.6 kpc of the Sun) to trace the nearby arms, recent observations have shown the interarm distance to be 2.5 ± 0.3 kpc, as measured from the inner edge of Sagittarius to the inner edge of Perseus, along the radial Sun–GC line (Fernandez, Figueras, & Torra 2001, their Fig. 4).

Figure 3 shows the four spiral arms in a plot of log (radius) versus angle from the Sun–GC axis. Such a plot unwraps the logarithmic spirals into straight lines. The area on the other side of the GC has been darkened as before (zona Galactica incognita). Data lying inside $r = 3$ kpc are not plotted since other physical phenomena are occurring there (bar and nucleus); ditto for data lying outside $r = 13$ kpc (warp and tides). The interarm distance S at the Sun is shown. The radio rotation measure (RM) distribution can give the pitch angle of magnetic field lines (parallel to the stellar arms), as well as the magnetic field direction in the Galaxy (e.g., Fig. 9 in Vallée 1997).

4.2. *Orion Spur*

Observationally, the Sun is located in the small local "Orion spur," roughly halfway between the large Perseus arm and the large Sagittarius arm.

In our model, it is impossible to claim that the local Orion Spur is itself a long bona fide spiral arm because the interarm distance would now become about half of our 2.5 kpc value ($r_2 - r_1 = 1.55$kpc; $r_\odot - r_1 = 0.94$ kpc), and this would make our home Galaxy have an interarm S about 50% smaller than observed in other nearby spiral galaxies of the same morphology at the same radial distance (greater than 2 kpc).

5. CONCLUSION AND FUTURE WORK

In this paper, the global parameters of the Milky Way as obtained from a meta-analysis ($\langle m \rangle$, $\langle p \rangle$) and from other sources (arm tangents, central bar P.A., Sun–GC distance) are employed in a preferred model to yield the best locations (radius, longitude) for the logarithmic spiral arms in the Milky Way disk. From the best fit, two predictions have been made, such as for the interarm separation S and the Sun's distance to the Sagittarius arm.

The main results are as follows:

1. Using the results published in the period 1995–2001, this metastudy covering 17 new papers shows that our home Galaxy has $m = 4$ arms, with a mean pitch angle $p = 12°$ inward to within 1° (Table 1).
2. These results in $\langle m \rangle$ and $\langle p \rangle$ corroborate and confirm those in an independent metastudy (Vallée 1995), and they show consistency in values and convergence in time (1980–2001).
3. With these two Galactic parameters ($\langle m \rangle$, $\langle p \rangle$), model fits have been made to the Galactic longitudes (to within 3°) tangent to the observed arms (Fig. 2), with arms starting near the two ends of the bar, yielding the model arm parameters ($r_0 = 2.3$kpc; $\theta_0 = 0°$).
4. These fits in r_0 and θ_0 corroborate and confirm those in an independent study (Ortiz & Lépine 1993), also showing consistency in values and convergence in time.
5. The model predicts the value of the interarm distance near the Sun, computed as $S = 2.5$ kpc (Fig. 3), and the Sun's distance to the Sagittarius arm (Table 2). The interarm prediction is difficult to compare to observational data but is close to the value found from recent well-calibrated Cepheids data.

The model here makes some predictions that differ substantially from the similar model of Ortiz & Lépine (1993) about the interarm distance S near the Sun, the Sun's distance to the Sagittarius arm, and the presence or absence of a central bar (see Table 2). However, there is a good agreement between the two models in the radial range from 3 to 6 kpc from the GC.

The mean values for m and p obtained from a single observational method are comparable to the mean values obtained from any other method. The distribution in m values is already quite narrow, with 15 studies (of 19) finding $m = 4$ (from Table 1). The distribution in p is large and could still be narrowed more in future studies (Fig. 1). A look at Figure 1 shows a large range in pitch angle values, from $p = 6°$ to 20° inward. Within the *same* observational method, the individual p values as found by different groups may differ by a large amount. Thus, the optical Cepheids method yields results in the range $p = 6°$ to $p = 14°$, depending on the $m = 2$, 4, or 6 value adopted. For Cepheids, it appears that a full calibration of the Cepheids data within the Gould Belt can have an important impact on the results (Fernandez et al. 2001). In contrast, the radio H I method yields results in the range $p = 11°$–$14°$ and $m = 4$, consistently.

I thank an anonymous referee for thoughtful suggestions.

REFERENCES

Amaral, L. H., & Lépine, J. R. 1997, MNRAS, 286, 885
Binney, J., Gerhard, O., Stark, A., Bally, J., & Uchida, K. 1991, MNRAS, 252, 210
Chen, W., Gehrels, N., Diehl, R., & Hartmann, D. 1996, A&AS, 120, 315
Deshpande, A. A. 1995, Bull. Astron. Soc. India, 23, 459
Drimmel, R. 2000, A&A, 358, L13
Efremov, Y. N. 1998, Astron. Astrophys. Trans., 15, 3
Elmegreen, B. G., Elmegreen, D. M., & Montenegro, L. 1992, ApJS, 79, 37
Englmaier, P., & Gerhard, O. 1999, MNRAS, 304, 512
Fernandez, D., Figueras, F., & Torra, J. 2001, A&A, 372, 833
Freudenreich, H. T. 1998, ApJ, 492, 495
Fux, R. 1999, A&A, 345, 787
———. 2001, A&A, 373, 511
Gerhard, O. E. 1999, in ASP Conf. Ser. 182, Galaxy Dynamics, ed. D. Merritt, J. A. Sellwood, & M. Valluri (San Francisco: ASP), 307
Grosbol, P. 1994, in Galactic Dynamics and N-Body Simulations, ed. G. Contopoulos, N. K. Spyrou, & L. Vlahos (Berlin: Springer), 101
Han, J. L., Manchester, R., & Qiao, G. J. 1999, MNRAS, 306, 371
Heiles, C. 1996, ApJ, 462, 316
Indrani, C., & Deshpande, A. A. 1999, NewA, 4, 33
Johnston, S., Koribalski, B., Weisberg, J. M., & Wilson, W. 2001, MNRAS, 322, 715

Lépine, J. R. D., Mishurov, Y. N., & Dedikov, S. Y. 2001, ApJ, 546, 234
Mishurov, Yu. N., & Zenina, I. A. 1999, A&A, 341, 81
Ollin, R. P., & Merrefield, M. R. 1998, MNRAS, 297, 943
Ortiz, R., & Lépine, J. R. D. 1993, A&A, 279, 90
Paczyński, B., & Stanek, K. L. 1998, ApJ, 494, L219
Reid, M. J. 1993, ARA&A, 31, 345
Sevenster, M. N. 1999, MNRAS, 310, 629
Steiman-Cameron, T. Y., Wolfire, M. G., & Hollenbach, D. J. 2001, BAAS, 32, 1391, 04.14
Vallée, J. P. 1995, ApJ, 454, 119
———. 1997, Fundam. Cosmic Phys., 19, 1
Vallenari, A., Bertelli, G., & Schmidtobreick, L. 2000, A&A, 361, 73